Preconditioned Iteration Method for the Nonlinear Space Fractional Complex Ginzburg-Landau Equation

Lu Zhang[1(✉)], Lei Chen[2], and Xiao Song[1]

[1] School of Mathematics and Statistics, Xuzhou University of Technology, Xuzhou 221018, Jiangsu, China
[2] School of Information Engineering, Xuzhou University of Technology, Xuzhou 221018, Jiangsu, China
chenlei@xzit.edu.cn

Abstract. In this work, we give a fast preconditioned numerical method to solve the discreted linear system, which is obtained from the nonlinear space fractional complex Ginzburg-Landau equation. The coefficient matrix of the discreted linear system is the sum of a complex diagonal matrix and a real Toeplitz matrix. The new method has a superiority in computation because we can use the circulant preconditioner and the fast Fourier transform (FFT) to solve the discreted linear system. Numerical examples are tested to illustrate the advantage of the preconditioned numerical method.

Keywords: Nonlinear fractional ginzburg-landau equation · Toeplitz matrix · Circulant preconditioner · Fast fourier transform

1 Introduction

In this work, we solve the nonlinear space fractional complex Ginzburg-Landau equation as follows [13]

$$\frac{\partial v}{\partial t} + (\nu_1 + \mathbf{i}\eta_1)(-\Delta)^{\frac{\beta}{2}} v + (\kappa_1 + \mathbf{i}\zeta_1)|v|^2 v - \gamma_1 v = 0, \tag{1}$$

$$v(x, 0) = v_0(x), \tag{2}$$

where $x \in \mathbb{R}$, $0 < t \leqslant T_1$, $\mathbf{i}$ is the imaginary unit, $1 < \beta \leqslant 2$, $v(x,t)$ is a complex-value function, $\nu_1 > 0$, $\kappa_1 > 0$, η_1, ζ_1, and γ_1 are real constants, and $v_0(x)$ is an initial function. Furthermore, the operator $(-\Delta)^{\frac{\beta}{2}} v(x,t)$ in (1) denotes the derivative operator $(1 < \beta \leqslant 2)$ [10] as follows

$$-(-\Delta)^{\frac{\beta}{2}} v(x,t) = -\frac{\frac{\partial^2}{\partial x^2} \int_{-\infty}^{\infty} |x-\xi|^{1-\beta} v(\xi, t) \mathrm{d}\xi}{2\cos(\frac{\beta\pi}{2})\Gamma(2-\beta)}. \tag{3}$$

Supported by the "Peiyu" Project from Xuzhou University of Technology (Grant Number XKY2019104).

H. Song and D. Jiang (Eds.): SIMUtools 2020, LNICST 370, pp. 351–362, 2021.
https://doi.org/10.1007/978-3-030-72795-6_29

The fractional Ginzburg-Landau equations have been used to describe a lot of physical phenomena; see [27,28,33,34] for example. In theory, some scholars have studied the fractional Ginzburg-Landau equations [11,30,35]. In the numerical computation, there exists few studies for the nonlinear fractional equations (1)–(2); see [13,28,36,40] and reference therein. Therefore, based on the extensive applied fields of these equations, it is interesting to study the numerical methods for solving the nonlinear fractional equations (1)–(2).

Recently, some new techniques are proposed to improve network routing and performance measurement [14,37,41]. Based on effective user behavior and traffic analysis approaches [5,6,23,24], we can design more effective scheduling strategies to raise resources utilization [7,17,18,38] and energy-efficiency [19,20]. To test new scheduling strategies, traffic must be reconstructed in test bed [15,16,21,22,31,39]. Fluid model is effective model to reconstruct the bursty data traffic. Furthermore, fractional differential equation can be used to build the fluid model. The main aim of our paper is to give a fast preconditioned numeical method to solve the discreted linear system, which is obtained from the nonlinear fractional equations (1)–(2). The superiority of our method is that in the process of solving the nonlinear fractional equations (1)–(2), we can fast solve the complex linear systems by using the circulant preconditioner and the FFT at each step due to the special structure of coefficient matrices.

2 A Finite Difference Scheme for the Fractional Equations

In this part, we use the linearized difference scheme [13] to discretize the the nonlinear fractional equations (1)–(2). And the fractional operator $(-\varDelta)^{\frac{\beta}{2}}$ is discretized in the nonlinear fractional equations (1)–(2) by the centered difference method [2] which is given as follows

$$\varDelta_{\hat{h}}^{\beta} v(x) = \frac{\sum\limits_{i=-\infty}^{+\infty} d_i^{(\beta)} v(x - i\hat{h})}{\hat{h}^{\beta}},$$

where $d_i^{(\beta)}$ can be obtained by the following formulation

$$d_i^{(\beta)} = \frac{(-1)^i \varGamma(\beta+1)}{\varGamma(\frac{\beta}{2}-i+1)\varGamma(\frac{\beta}{2}+i+1)}, \quad i \in \mathbb{Z}. \tag{4}$$

In the following, we give the numerical finite difference scheme of the nonlinear fractional equations (1)–(2) in $\varPi = [a_1, a_2]$. We separate the domain $\{(x,t) | a_1 \leqslant x \leqslant a_2, 0 \leqslant t \leqslant T_1\}$ by a uniform grid $\{(x_j, t_i) | x_j = a_1 + j\hat{h}, t_i = i\hat{\tau}, j = 0, \ldots, M_1, i = 0, \ldots, N_1\}$, with $\hat{h} = \frac{a_2 - a_1}{M_1}, \hat{\tau} = \frac{T_1}{N_1}$, where M_1 and N_1 are two positive integers.

Denote v_j^i the numerical solution to the exact solution $v(x_j, t_i)$. For any grid function $v^i = (v_0^i, v_1^i, \ldots, v_{M_1}^i)$, According to [13], we define

$$v_j^{\tilde{i}} = \frac{v_j^{i+1} + v_j^{i-1}}{2}, \ \delta_t v_j^i = \frac{v_j^{i+1} - v_j^{i-1}}{2\hat{\tau}}.$$

Denote

$$\tilde{Z}_{\hat{h}}^0 = \{V|V = \{V_j\}, j = 0, 1, \ldots, M_1, V_0 = V_{M_1} = 0\}.$$

For any $v \in \tilde{Z}_{\hat{h}}^0$, we have

$$\Delta_{\hat{h}}^{\beta} v_j = \frac{1}{\hat{h}^{\beta}} \sum_{i=j-1}^{j-M_1+1} d_i^{(\beta)} v_{j-i}.$$

The linearized implicit method [13] for the nonlinear fractional equations (1)–(2) in $\Pi = [a_1, a_2]$ is as follows

$$\begin{aligned} &\delta_t v_j^{i+1} + (\nu_1 + \mathbf{i}\eta_1)\Delta_{\hat{h}}^{\beta} v_j^{\tilde{i}} + (\kappa_1 + \mathbf{i}\zeta_1)|v_j^i|^2 v_j^{\tilde{i}} - \gamma_1 v_j^{\tilde{i}} = 0, \\ &0 < j < M_1, \ 1 < i < N_1, \end{aligned} \tag{5}$$

$$v_j^0 = v_0(x_j), 0 < j < M_1, \tag{6}$$

$$v_0^i = v_{M_1}^i = 0, 0 \leqslant i \leqslant N_1. \tag{7}$$

In the practical computation, we can obtain v^1 from the following scheme [13]

$$v_j^1 = v_j^0 - \hat{\tau}\left((\nu_1 + \mathbf{i}\eta_1)\Delta_{\hat{h}}^{\beta} v_j^0 + (\kappa_1 + \mathbf{i}\zeta_1)|v_j^0|^2 v_j^0 - \gamma_1 v_j^0\right), 0 < j < M_1. \tag{8}$$

Denote

$$\tilde{v}^i = [v_1^i, \ldots, v_{M_1-1}^i]^T,$$

$$Q_1^1 = (1 + \gamma_1\hat{\tau})I - \hat{\tau}(\kappa_1 + \mathbf{i}\zeta_1)\begin{bmatrix} |v_1^0|^2 & 0 & \ldots & 0 \\ 0 & |v_2^0|^2 & \ldots & 0 \\ \vdots & \vdots & \ddots & \vdots \\ 0 & 0 & \ldots & |v_{M_1-1}^0|^2 \end{bmatrix},$$

$$Q_1^i = (1 - \gamma_1\hat{\tau})I + \hat{\tau}(\kappa_1 + \mathbf{i}\zeta_1)\begin{bmatrix} |v_1^i|^2 & 0 & \ldots & 0 \\ 0 & |v_2^i|^2 & \ldots & 0 \\ \vdots & \vdots & \ddots & \vdots \\ 0 & 0 & \ldots & |v_{M_1-1}^i|^2 \end{bmatrix},$$

$$Q_2^i = (1 + \gamma_1\hat{\tau})I - \hat{\tau}(\kappa_1 + \mathbf{i}\zeta_1)\begin{bmatrix} |v_1^i|^2 & 0 & \ldots & 0 \\ 0 & |v_2^i|^2 & \ldots & 0 \\ \vdots & \vdots & \ddots & \vdots \\ 0 & 0 & \ldots & |v_{M_1-1}^i|^2 \end{bmatrix},$$

and

$$D_\beta = \begin{bmatrix} d_0^{(\beta)} & d_1^{(\beta)} & d_2^{(\beta)} & \cdots & d_{M_1-2}^{(\beta)} & d_{M_1-1}^{(\beta)} \\ d_1^{(\beta)} & d_0^{(\beta)} & d_1^{(\beta)} & \cdots & \cdots & d_{M_1-2}^{(\beta)} \\ d_2^{(\beta)} & d_1^{(\beta)} & d_0^{(\beta)} & \ddots & \ddots & \vdots \\ \vdots & \ddots & \ddots & \ddots & \ddots & d_2^{(\beta)} \\ d_{M_1-2}^{(\beta)} & \ddots & \ddots & \ddots & d_0^{(\beta)} & d_1^{(\beta)} \\ d_{M_1-1}^{(\beta)} & d_{M_1-2}^{(\beta)} & \cdots & d_2^{(\beta)} & d_1^{(\beta)} & d_0^{(\beta)} \end{bmatrix}, \tag{9}$$

then the linearized implicit method (5)–(8) has the following formulation

$$\tilde{v}^1 = (Q_1^1 - (\nu_1 + \mathbf{i}\eta_1)A_\beta)\tilde{v}^0, \tag{10}$$

$$\left(\frac{Q_1^i}{\nu_1 + \mathbf{i}\eta_1} + A_\beta\right)\tilde{v}^{i+1} = \left(\frac{Q_2^i}{\nu_1 + \mathbf{i}\eta_1} - A_\beta\right)\tilde{v}^{i-1}, 1 < i < N_1, \tag{11}$$

where $A_\beta = \frac{\hat{\tau}}{\hat{h}^\beta} D_\beta$.

3 A Preconditioned Iterative Method for the Linearized Implicit Method

In this section, we propose a fast preconditioned GMRES (PGMRES) method [32] where the Strang preconditioner [3] is used to solve the linear system in the matrix-vector form (10)–(11).

3.1 Toeplitz Matrix and GMRES Method

It is known that an $n_1 \times n_1$ Toeplitz matrix B_{n_1} satisfies $(B_{n_1})_{ij} = b_{i-j}$ for $i, j = 1, 2, \ldots, n_1$. And the Toeplitz system is as follows

$$B_{n_1} u = \tilde{b},$$

where $\tilde{b}$ is a given vector. Toeplitz systems are widely used in various fields; see [1,4,8,12,25,26,29] for example.

An $n_1 \times n_1$ circulant matrix C_{n_1} is a Toeplitz matrix and its elements satisfy $c_{-j} = c_{n_1-j}$ for $1 \leqslant j \leqslant n_1 - 1$. According to the result of the reference [9], it is worth noting that if we want to compute the matrix-vector products $C_{n_1}u$ and $C_{n_1}^{-1}u$ efficiently by the fast Fourier transform, the computation complexity will be $\mathcal{O}(n_1 \log n_1)$ operations. We also note that [3] one can compute the matrix-vector product $B_{n_1}u$ by the FFT in $\mathcal{O}(2n_1 \log(2n_1))$. These important properties could be exploited to fast solve the linear system in the matrix-vector form (10)–(11).

The GMRES method [32] is a very popular numerical iterative method for solving the following non-Hermitian linear systems

$$Au = \tilde{b},$$

where A is a non-Hermitian matrix. However, the convergent rate of the GMRES method is very slow in general because of the large condition number of the coefficient matrix of linear systems. To deal with this drawback, we can use the preconditioned matrix to accelerate the convergent rate of the GMRES method. Please refer to [32] for the PGMRES method.

3.2 A Preconditioner for the Linearized Implicit Difference Scheme

From Sect. 2, It is noted that the matrix A_β is a Toeplitz matrix in the matrix-vector form (10)–(11) of the linearized implicit difference scheme. According to Sect. 3.1, it is seen that for an $M_1 \times M_1$ Toeplitz matrix B_{M_1}, we could store this matrix in $\mathcal{O}(M_1)$ of memory and compute the matrix-vector product $B_{M_1}u$ in $\mathcal{O}(M_1 \log M_1)$ by using the FFT. On the other hand, it is worth noting that the coefficient matrix $\frac{Q_1^i}{\nu_1+\mathbf{i}\eta_1} + A_\beta$ of linear systems (11) is non-Hermitian. Therefore, we exploit the PGMRES method to solve the linear systems of the linearized implicit difference scheme (10)–(11). Strang's circulant matrix [3,4] is a circulant matrix and can be applied to accelerate the convergent rate of the GMRES method.

According to the linear system (11), we note that the matrix $\frac{Q_1^i}{\nu_1+\mathbf{i}\eta_1}+A_\beta$ is not a Toeplitz matrix. In this situation, standard Strang's circulant preconditioner can not be used to solve the linear systems (11) directly. To deal with this problem, we will give a new effective preconditioner for the coefficient matrix $\frac{Q_1^i}{\nu_1+\mathbf{i}\eta_1} + A_\beta$.

For the coefficient matrix

$$\frac{Q_1^i}{\nu_1+\mathbf{i}\eta_1} + A_\beta$$

in (11), let

$$\tilde{a} = \frac{1}{M_1-1}\sum_{j=1}^{M_1-1} \frac{1-\gamma_1\hat{\tau}+\hat{\tau}(\kappa_1+\mathbf{i}\zeta_1)|v_j^i|^2}{\nu_1+\mathbf{i}\eta_1},$$

then the preconditioned matrix is $P = \tilde{a}I + s(A_\beta)$ for coefficient matrix $\frac{Q_1^i}{\nu_1+\mathbf{i}\eta_1} + A_\beta$, where $s(A_\beta)$ denotes the Strang circulant preconditioner for the Toeplitz matrix A_β. Therefore, we obtain a circulant matrix P. In the next section, we will see that the proposed preconditioner is very effective for the PGMRES method.

4 Numerical Examples

In this part, we carry out two numerical examples for the nonlinear fractional equations (1)–(2). We will show the computational advantage of the proposed proconditioner for GMRES method. We denote "GE" by the direct method, which is implemented by left divided in MATLAB. For the PGMRES method with Strang's circulant preconditioner, we denote by "CPGMRES". We stop the PGMRES method if the following condition satisfies

$$\frac{\|\mathrm{res}^k\|_2}{\|\mathrm{res}^0\|_2} < 10^{-7},$$

where res^k denotes the k-th residual vector for the PGMRES method. In the tables of numerical examples, "Icpu" is the computational time with seconds for GE and CPGMRES, and "It" is the numbers of iterations for CPGMRES.

Example 1. In the first example, the parameters in the nonlinear fractional Eq. (1) and (2) are same as these of Example 1 in [13].

Furthermore, similar to [13], for $1 < \beta < 2$, we calculate the exact solution v with $\hat{\tau} = \frac{1}{256}$ and $\hat{h} = \frac{1}{256}$. We use the error Err$= v - V(\hat{h}, \hat{\tau})$ as the numerical accuracy at $T_1 = 1$ with l^∞-norm.

Table 1. Numerical results for Example 1

β	$(\hat{\tau}, \hat{h})$	CPGMRES			GE	
		Err_1	It	Icpu	Err_2	Icpu
1.2	$(\frac{1}{8}, \frac{1}{8})$	9.4621e−3	6.0	0.0150	9.4621e−3	0.0160
	$(\frac{1}{16}, \frac{1}{16})$	2.3726e−3	5.0	0.0160	2.3725e−3	0.1090
	$(\frac{1}{32}, \frac{1}{32})$	5.8698e−4	5.0	0.0940	5.8697e−4	1.3910
	$(\frac{1}{64}, \frac{1}{64})$	1.4043e−4	4.0	0.2340	1.3980e−4	16.4700
	$(\frac{1}{128}, \frac{1}{128})$	2.8145e−5	4.0	1.0470	2.7961e−5	187.0640
1.5	$(\frac{1}{8}, \frac{1}{8})$	9.4826e−3	6.0	0.0160	9.4825e−3	0.0160
	$(\frac{1}{16}, \frac{1}{16})$	2.3620e−3	5.0	0.0160	2.3620e−3	0.1090
	$(\frac{1}{32}, \frac{1}{32})$	5.8343e−4	5.0	0.0930	5.8342e−4	1.3750
	$(\frac{1}{64}, \frac{1}{64})$	1.3866e−4	4.3	0.2660	1.3889e−4	16.2380
	$(\frac{1}{128}, \frac{1}{128})$	2.7810e−5	4.0	1.0320	2.7760e−5	184.3910
1.8	$(\frac{1}{8}, \frac{1}{8})$	8.2560e−3	6.0	0.0160	8.2560e−3	0.0160
	$(\frac{1}{16}, \frac{1}{16})$	2.0541e−3	5.0	0.0150	2.0540e−3	0.1400
	$(\frac{1}{32}, \frac{1}{32})$	5.0720e−4	5.0	0.0940	5.0720e−4	1.4070
	$(\frac{1}{64}, \frac{1}{64})$	1.2084e−4	4.8	0.2810	1.2074e−4	16.6880
	$(\frac{1}{128}, \frac{1}{128})$	2.4174e−5	4.2	1.1100	2.4136e−5	187.5820

We list the numerical results in Table 1. In this table, Err_1 and Err_2 are calculated by the CPGMRES method and the GE method, respectively. From the computational results of Table 1, it can be seen that Err_1 and Err_2 of the CPGMRES method and the GE method are almost the same. However, if the order of the coefficient matrix is very large in the complex linear systems (10)–(11), the computational times of the GE method are much more than these of the CPGMRES method. Furthermore, according to Table 1, we can see that the numbers of iterations for the CPGMRES method do not change when the order of the coefficient matrix increases. On the other hand, Fig. 1, 2, 3 show the distribution of the eigenvalues for the matrices $\frac{Q_1^i}{\nu_1+\mathbf{i}\eta_1}+A_\beta$ and $P^{-1}(\frac{Q_1^i}{\nu_1+\mathbf{i}\eta_1}+A_\beta)$ at $T_1=1$, respectively, when the order of the matrix is 640, and $\beta=1.2,\ 1.5,\ 1.8$. In these figures, the blue points show that most of the eigenvalues of the matrix $P^{-1}(\frac{Q_1^i}{\nu_1+\mathbf{i}\eta_1}+A_\beta)$ approach to 1, while the eigenvalues of the matrix $\frac{Q_1^i}{\nu_1+\mathbf{i}\eta_1}+A_\beta$ do not approach to 1. These figures show that our new circulant preconditioner is very effective for solving the complex linear systems (10)–(11).

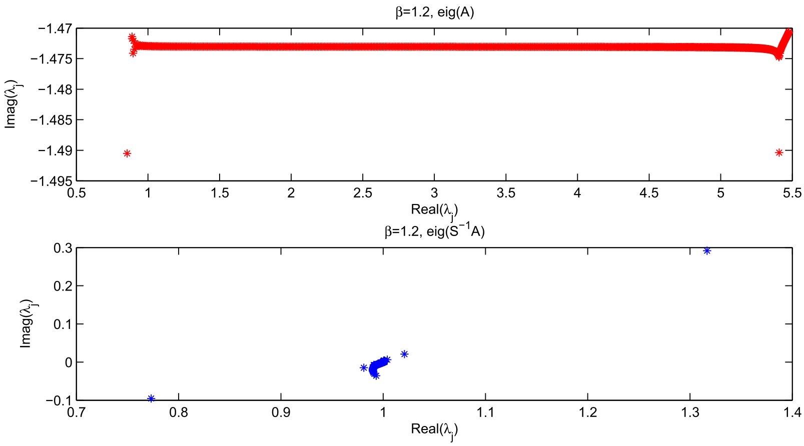

Fig. 1. Example 1: Spectrum of $\frac{Q_1^i}{\nu_1+\mathbf{i}\eta_1}+A_\beta$ (upper) and $P^{-1}(\frac{Q_1^i}{\nu_1+\mathbf{i}\eta_1}+A_\beta)$(lower), when $\beta=1.2$.

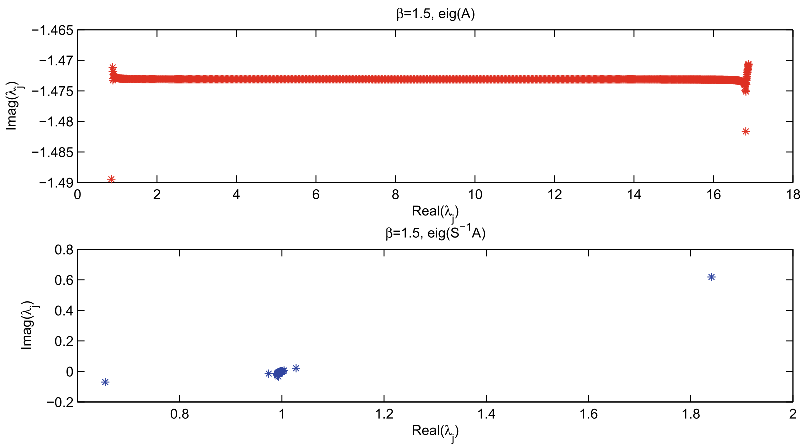

Fig. 2. Example 1: Spectrum of $\frac{Q_1^i}{\nu_1+\mathbf{i}\eta_1}+A_\beta$ (upper) and $P^{-1}(\frac{Q_1^i}{\nu_1+\mathbf{i}\eta_1}+A_\beta)$(lower), when $\beta=1.5$.

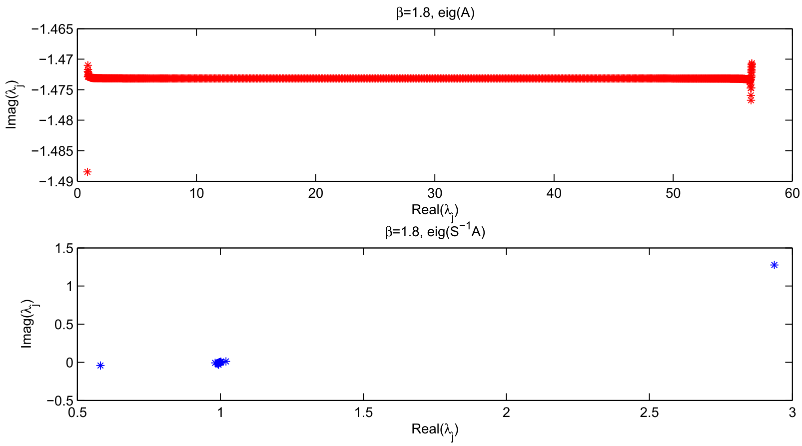

Fig. 3. Example 1: Spectrum of $\frac{Q_1^i}{\nu_1+\mathbf{i}\eta_1}+A_\beta$ (upper) and $P^{-1}(\frac{Q_1^i}{\nu_1+\mathbf{i}\eta_1}+A_\beta)$(lower), when $\beta=1.8$.

Example 2. In the second example, the parameters in the nonlinear fractional equations (1) and (2) are same as these of Example 2 in [13]. Furthermore, we also compute the exact solution v with $\hat{\tau}=\frac{1}{256}$ and $\hat{h}=\frac{1}{256}$.

Table 2. Numerical results for Example 2

β	$(\hat{\tau},\hat{h})$	CPGMRES			GE	
		Err_1	It	Icpu	Err_2	Icpu
1.2	$(\frac{1}{8},\frac{1}{8})$	3.3383e−1	8.1	0.0210	3.3383e−1	0.0190
	$(\frac{1}{16},\frac{1}{16})$	9.2876e−2	6.9	0.0340	9.2876e−2	0.1150
	$(\frac{1}{32},\frac{1}{32})$	2.3571e−2	6.1	0.1230	2.3571e−2	1.4230
	$(\frac{1}{64},\frac{1}{64})$	5.6471e−3	6.0	0.3600	5.6472e−3	16.7920
	$(\frac{1}{128},\frac{1}{128})$	1.1312e−3	5.2	1.3890	1.1311e−3	185.7270
1.5	$(\frac{1}{8},\frac{1}{8})$	3.3573e−1	8.0	0.0210	3.3573e−1	0.0140
	$(\frac{1}{16},\frac{1}{16})$	8.4910e−2	7.1	0.0360	8.4910e−2	0.1220
	$(\frac{1}{32},\frac{1}{32})$	2.0546e−2	6.3	0.1160	2.0546e−3	1.4110
	$(\frac{1}{64},\frac{1}{64})$	4.8463e−3	6.0	0.3530	4.8463e−3	16.5600
	$(\frac{1}{128},\frac{1}{128})$	9.6640e−4	5.9	1.5340	9.6657e−4	186.4660
1.8	$(\frac{1}{8},\frac{1}{8})$	5.1805e−1	8.0	0.0220	5.1805e−1	0.0200
	$(\frac{1}{16},\frac{1}{16})$	1.2586e−1	7.1	0.0370	1.2586e−1	0.1220
	$(\frac{1}{32},\frac{1}{32})$	2.9409e−2	6.3	0.1170	2.9409e−2	1.3890
	$(\frac{1}{64},\frac{1}{64})$	6.8588e−3	6.0	0.3560	6.8588e−3	17.7910
	$(\frac{1}{128},\frac{1}{128})$	1.3639e−3	5.9	1.6640	1.3639e−3	194.5380

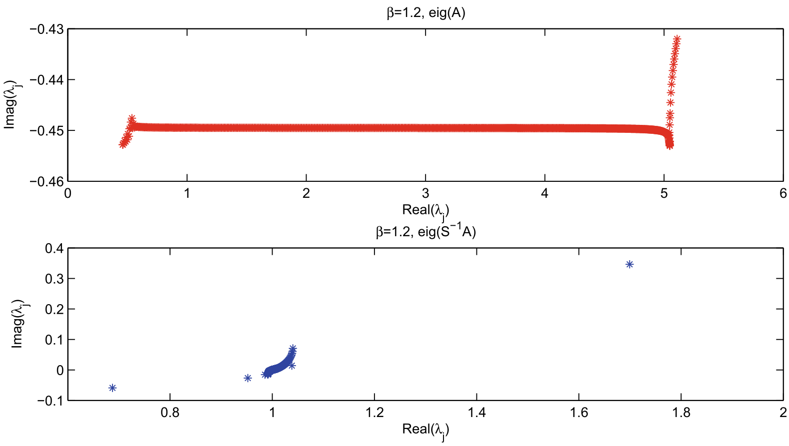

Fig. 4. Example 2: Spectrum of $\frac{Q_1^i}{\nu_1+\mathbf{i}\eta_1} + A_\beta$ (upper) and $P^{-1}(\frac{Q_1^i}{\nu_1+\mathbf{i}\eta_1} + A_\beta)$(lower), when $\beta = 1.2$.

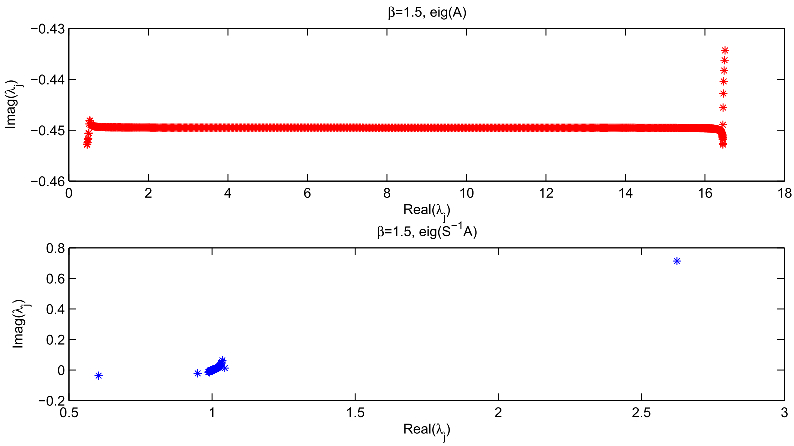

Fig. 5. Example 2: Spectrum of $\frac{Q_1^i}{\nu_1+\mathbf{i}\eta_1} + A_\beta$ (upper) and $P^{-1}(\frac{Q_1^i}{\nu_1+\mathbf{i}\eta_1} + A_\beta)$(lower), when $\beta = 1.5$.

Table 2 gives the numerical results and Fig. 4, 5, 6 show the distribution of the eigenvalues for the matrices $\frac{Q_1^i}{\nu_1+\mathbf{i}\eta_1} + A_\beta$ and $P^{-1}(\frac{Q_1^i}{\nu_1+\mathbf{i}\eta_1} + A_\beta)$ at $T_1 = 1$, respectively, when the order of the matrix is 640, and $\beta = 1.2,\ 1.5,\ 1.8$. Similar to Example 1, the numerical results and figures indicate the advantage of the proposed circulant preconditioner.

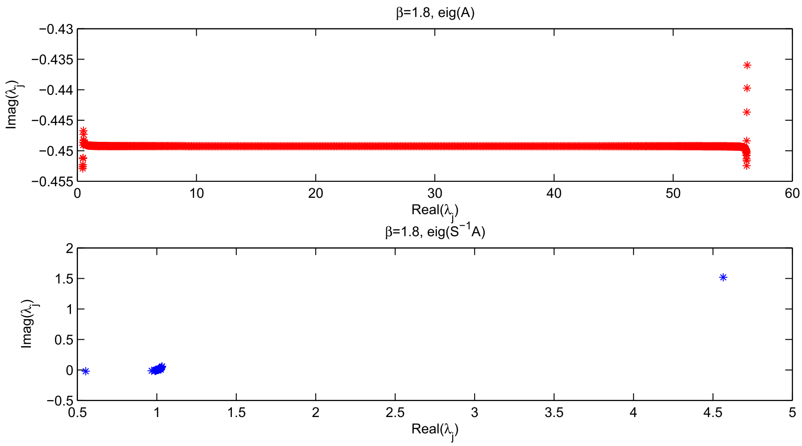

Fig. 6. Example 2: Spectrum of $\frac{Q_1^i}{\nu_1+\mathbf{i}\eta_1}+A_\beta$ (upper) and $P^{-1}(\frac{Q_1^i}{\nu_1+\mathbf{i}\eta_1}+A_\beta)$(lower), when $\beta=1.8$.

5 Conclusion and Future Work

In this paper, we have given a fast preconditioned numerical method to solve the discreted linear system, which is obtained from the nonlinear fractional equations. Due to the special structure of coefficient matrix of linear system, we propose an effective circulant preconditioner. Numerical examples well verify the preconditioned numerical method.

References

1. Bunch, J.R.: Stability of methods for solving Toeplitz systems of equations. SIAM J. Sci. Stat. Comput. **6**, 349–364 (1985)
2. Çelik, C., Duman, M.: Crank-Nicolson method for the fractional diffusion equation with the Riesz fractional derivative. J. Comput. Phys. **231**, 1743–1750 (2012)
3. Chan, R., Jin, X.: An Introduction to Iterative Toeplitz Solvers. SIAM, Philadelphia (2007)
4. Chan, R., Ng, M.: Conjugate gradient methods for Toeplitz systems. SIAM Rev. **38**, 427–482 (1996)
5. Chen, L., Jiang, D., Bao, R., Xiong, J., Liu, F., Bei, L.: MIMO Scheduling effectiveness analysis for bursty data service from view of QoE. Chin. J. Electron **26**(5), 1079–1085 (2017)
6. Chen, L., Jiang, D., Song, H., Wang, P., Bao, R., Zhang, K., Li, Y.: A lightweight end-side user experience data collection system for quality evaluation of multimedia communications. IEEE Access **6**(1), 15408–15419 (2018)
7. Chen, L., Zhang, L.: Spectral efficiency analysis for massive MIMO system Under QoS constraint: an effective capacity perspective. Mobile Netw. Appl. (2020). https://doi.org/10.1007/s11036-019-01414-4
8. Ching, W.-K.: Iterative Methods for Queuing and Manufacturing Systems. Springer-Verlag, London (2001)

9. Davis, P.: Circulant Matrices, 2nd edn. AMS Chelsea, Providence, RI (1994)
10. Gorenflo, R., Mainardi, F.: Random walk models for space-fractional diffusion processes. Fractional Calc. Appl. Anal. **1**(2), 167–191 (1998)
11. Guo, B.-L., Huo, Z.-H.: Well-posedness for the nonlinear fractional Schrödinger equation and inviscid limit behavior of solution for the fractional Ginzburg-Landau equation. Fract. Calc. Appl. Anal. **16**(1), 226–242 (2012)
12. Hansen, P.C., Nagy, J.G., O'Leary, D.P.: Deblurring Images: Matrices, Spectra, and Filtering. SIAM, Philadelphia (2006)
13. He, D., Pan, K.: An unconditionally stable linearized difference scheme for the fractional Ginzburg-Landau equation. Numer. Algor. **79**, 899–925 (2018)
14. Huo, L., Jiang, D., Lv, Z., et al.: An intelligent optimization-based traffic information acquirement approach to software-defined networking. Comput. Intell. **1–21** (2019)
15. Huo, L., Jiang, D., Qi, S., et al.: An AI-based adaptive cognitive modeling and measurement method of network traffic for EIS. Mob. Netw. Appl. 1–11 (2019)
16. Huo, L., Jiang, D., Zhu, X., et al.: An SDN-based fine-grained measurement and modeling approach to vehicular communication network traffic. Int. J. Commun. Syst. e4092 (2019)
17. Jiang, D., Huo, L., Lv, Z., et al.: A joint multi-criteria utility-based network selection approach for vehicle-to-infrastructure networking. IEEE Trans. Intell. Transp. Syst. **19**(10), 3305–3319 (2018)
18. Jiang, D., Zhang, P., Lv, Z., et al.: Energy-efficient multi-constraint routing algorithm with load balancing for smart city applications. IEEE Internet Things J. **3**(6), 1437–1447 (2016)
19. Jiang, D., Li, W., Lv, H.: An energy-efficient cooperative multicast routing in multi-hop wireless networks for smart medical applications. Neurocomputing **220**, 160–169 (2017)
20. Jiang, D., Wang, Y., Lv, Z., et al.: Intelligent Optimization-based reliable energy-efficient networking in cloud services for IIoT networks. IEEE J. Select. Areas Commun. (2019)
21. Jiang, D., Wang, W., Shi, L., et al.: A compressive sensing-based approach to end-to-end network traffic reconstruction. IEEE Trans. Netw. Sci. Eng. **5**(3), 1–12 (2018)
22. Jiang, D., Huo, L., Li, Y.: Fine-granularity inference and estimations to network traffic for SDN. Plos One **13**(5), 1–23 (2018)
23. Jiang, D., Wang, Y., Lv, Z., et al.: Big data analysis-based network behavior insight of cellular networks for industry 4.0 applications. IEEE Trans. Ind. Inform. **16**(2), 1310–1320 (2020)
24. Jiang, D., Huo, L., Song, H.: Rethinking behaviors and activities of base stations in mobile cellular networks based on big data analysis. IEEE Trans. Netw. Sci. Eng. **1**(1), 1–12 (2018)
25. Jin, X.-Q.: Developments and Applications of Block Toeplitz Iterative Solvers. The Netherlands, and Science Press, Beijing, China, Kluwer Academic Publishers, Dordrecht (2002)
26. Kailath, T., Sayed, A.H. (eds.): Fast Reliable Algorithms for Matrices with Structure. SIAM, Philadelphia (1999)
27. Milovanov, A., Rasmussen, J.: Fractional generalization of the Ginzburg-Landau equation: an unconventional approach to critical phenomena in complex media. Phys. Lett. **337**, 75–80 (2005)

28. Mvogo, A., Tambue, A., Ben-Bolie, G., Kofane, T.: Localized numerical impulse solutions in diffuse neural networks modeled by the complex fractional Ginzburg-Landau equation. Commun. Nonlinear Sci. **39**, 396–410 (2016)
29. Ng, M.K.: Iterative Methods for Toeplitz Systems. Oxford University Press, Oxford, UK (2004)
30. Pu, X., Guo, B.: Well-posedness and dynamics for the fractional Ginzburg-Landau equation. Appl. Anal. **92**, 318–334 (2013)
31. Qi, S., Jiang, D., Huo, L.: A prediction approach to end-to-end traffic in space information networks. Mob. Netw. Appl. 1–10 (2019)
32. Saad, Y.: Iterative Methods for Sparse Linear Systems. SIAM, Philadelphia (2003)
33. Tarasov, V., Zaslavsky, G.: Fractional Ginzburg-Landau equation for fractal media. Phys. **354**, 249–261 (2005)
34. Tarasov, V., Zaslavsky, G.: Fractional dynamics of coupled oscillators with long-range interaction. Chaos **16**(2), 023110 (2006)
35. Tarasov, V.: Psi-series solution of fractional Ginzburg-Landau equation. J. Phys. A-Math. Gen. **39**, 8395–8407 (2006)
36. Wang, P., Huang, C.: An implicit midpoint difference scheme for the fractional Ginzburg-Landau equation. J. Comput. Phys. **312**, 31–49 (2016)
37. Wang, F., Jiang, D., Qi, S.: An adaptive routing algorithm for integrated information networks. China Commun. **7**(1), 196–207 (2019)
38. Wang, F., Jiang, D., Qi, S., et al.: A dynamic resource scheduling scheme in edge computing satellite networks. Mob. Netw. Appl. 1–12 (2019)
39. Wang, Y., Jiang, D., Huo, L., et al.: A new traffic prediction algorithm to software defined networking. Mob. Netw. Appl. 1–10 (2019)
40. Wang, P., Huang, C.: An efficient fourth-order in space difference scheme for the nonlinear fractional Ginzburg-Landau equation. BIT **58**, 783–805 (2018)
41. Zhang, K., Chen, L., An, Y., et al.: A QoE test system for vehicular voice cloud services. Mobile Netw. Appl. (2019). https://doi.org/10.1007/s11036-019-01415-3